Molecular Crystals and Liquid Crystals Science and Technology. Section A. Molecular Crystals and Liquid Crystals

Publication details, including instructions for authors and subscription information:
http://www.tandfonline.com/loi/gmcl19

Coarsening Dynamics in Nematic Liquid Crystals

B. Yurke [a] , A. N. Pargellis [a] & N. Turok [b]

[a] AT&T - Bell Laboratories, Murray Hill, NJ, 07974

[b] Joseph Henry Laboratories, Princeton University, Princeton, NJ, 08544

Version of record first published: 04 Oct 2006.

To cite this article: B. Yurke , A. N. Pargellis & N. Turok (1992): Coarsening Dynamics in Nematic Liquid Crystals, Molecular Crystals and Liquid Crystals Science and Technology. Section A. Molecular Crystals and Liquid Crystals, 222:1, 195-203

To link to this article: http://dx.doi.org/10.1080/15421409208048693

Mol. Cryst. Liq. Cryst. 1992, Vol. 222, pp. 195–203
Reprints available directly from the publisher
Photocopying permitted by license only

Printed in the United States of America

Coarsening Dynamics in Nematic Liquid Crystals

B. Yurke[1], A. N. Pargellis[1], N. Turok[2]

[1] *AT&T - Bell Laboratories, Murray Hill, NJ 07974*
[2] *Joseph Henry Laboratories, Princeton University, Princeton, NJ 08544*

(Received October 10, 1991)

There is considerable interest in the dynamics of topological defects formed during a symmetry breaking phase transition in fields as diverse as condensed matter physics, particle physics and cosmology. Liquid crystals, with their many symmetry breaking phase transitions are ideal materials for such studies. Here we report on light transmission studies of the coarsening of three-dimensional defect tangles in uniaxial nematic liquid crystals subjected to a sudden pressure jump from the isotropic phase to the nematic phase. We have verified that the type 1/2 disclination line density, as a function of time, scales as $t^{-\nu}$ with $\nu = 1.0 \pm 0.1$ over four decades in time. The transmitted light intensity exhibits two distinct scaling regimes depending on whether propagation without scattering or diffusive propagation with multiple scattering dominates the light reaching the detector.

A system subjected to a rapid transition from a phase of high symmetry to a phase of lower symmetry will generate a tangle of topological defects. The resulting nonequilibrium configuration then relaxes toward equilibrium. As the system anneals the defect density decays with time and the system is said to coarsen. The dynamics of this process has become a topic of considerable interest in fields as diverse as condensed matter physics, particle physics and cosmology [1]. In condensed matter physics most of the activity has concentrated on predicting and measuring the scaling laws associated with the relaxation process [2-5]. Although much of this work has concentrated on systems whose topologial defects are domain walls, interest in systems exhibiting other kinds of topological defects has recently grown [6-13]. In cosmology, topological defects generated during symmetry breaking phase transitions have been invoked to explain the distribution of luminous matter in the universe [14-17]. Recently, topological defects generated at the time the universe underwent electroweak symmetry breaking have been invoked to explain the observed matter-antimatter asymmetry in the universe [18-21].

Liquid crystals, which exhibit a variety of symmetry breaking phase transitions, are particularly suitable for studies of the coarsening dynamics of defect tangles. Work, so far, has concentrated on the coarsening in nematic liquid crystals. The phase transition from the isotropic phase to the uniaxial nematic phase involves the breaking of global SO(3) symmetry to O(2). The vacuum manifold consists of the projective 2-sphere. The topological defects [22-24] generated in such a transition include type 1/2 disclination lines belonging to the π_1 homotopy class, hedgehogs or monopoles belonging to the π_2 homotopy class, and π_3 defects which are referred to as texture defects. Of these defects, the type 1/2 disclination lines are produced in greatest abundance during a sudden phase transition of bulk nematic from the isotropic to nematic phase. The density of line defects ρ_s in a three-dimensional tangle is expected to scale with time [8,13] as $t^{-\nu}$. Arguments have been put forth that the scaling exponent ν is 1. Coarsening studies have been carried out for thin films of both thermotropic [25-27] and polymer [28,29] nematic liquid crystals subjected to rapid temperature quenches. The scaling exponent ν for these two-dimensional systems depends on the boundary conditions imposed on the surfaces of the film. Recently we have studied the dynamics of three-dimensional defect tangles generated in nematic liquid crystals subjected to sudden pressure jumps from the isotropic phase to the nematic phase [30]. In our initial studies, the disclination line density was measured directly from video images of the defect tangle. This technique is limited to defect tangles that have coarsened sufficiently that background defects are no longer obscured by foreground defects. Finite size effects also place a long time limit, since boundary effects become important when the system has coarsened to the point where the average spacing between defect lines is comparable to spacing between the walls of the cell. Because of these limitations we could follow the coarsening for only one decade in time using video microscopy. Here we report on light transmission studies that have allowed us to follow the coarsening for four decades in time.

Light propagation through our sample cell exhibits two distinct scaling regimes which we now describe. To aid the discussion we will refer to the window, through which light enters the cell containing the liquid crystal, as the entrance window. The window through which the transmitted light leaves the cell will be referred to as the exit window. Defects provide scattering sites for light propagating through the cell. Shortly after the phase transition, when the defect density is high, the mean free path for the light is short compared to the cell thickness L. In this case the light propagates diffusively, executing a random walk. Most of the light diffuses back out through the entrance window. Assuming that there is negligible absorption of light by the medium, the intensity I of the light that diffuses to the exit window is proportional to the mean free path [31] and inversely proportional to the defect density,

$$I \propto 1/\rho_s \, . \tag{1}$$

Since the density of line defects ρ_s is expected to scale as t^{-1},

$$\rho_s \propto t^{-1} \, , \tag{2}$$

one expects the transmitted light intensity to be proportional to time at early times:

$$I \propto t \ . \tag{3}$$

At late times when the defect density is low very little light propagates through the cell diffusively. In this case, the defects serve to scatter light out of the light beam. Consequently the light propagating through the cell is given by the Lambert-Beer law

$$I = I_0 e^{-\alpha L} \tag{4}$$

where I_0 is the initial light intensity and α is the amount of light per unit length that is scattered out of the light beam. The light attenuation per unit length α is proportional to the defect density ρ_s. It thus follows that $-\ln(I/I_0)$ is a measure of ρ_s,

$$\rho_s \propto -\ln(I/I_0) \ . \tag{5}$$

Consequently, one expects $-\ln(I/I_0)$ to scale as

$$-\ln(I/I_0) \propto t^{-1} \ . \tag{6}$$

It is the scaling laws, Eq.(3) and Eq.(6) that we tested in the experiment described here. The liquid crystal used in these experiments, trans(trans)-4-methoxy-4'-n-pentyl-1,1'-bicyclohexyl, (Merck, CCH-501 or ZLI-3005), was chosen for its low optical anisotropy, $\Delta n = 0.027$, in order to reduce problems associated with light scattered from director field fluctuations. The optical anisotropy of this material is a factor of 5 smaller then typical optical anisotropies for thermotropic liquid crystals. The liquid crystal was housed inside a heated pressure cell with the entrance and exit windows arranged to allow for the observation of the defect tangle via transmission microscopy. The window appertures were 3 mm in diameter and the distance between the windows was 450 ± 50 μm. The windows were made of glass coated with homeotropic alignment material. The temperature of the liquid crystal was measured using a type K thermocouple projecting into the cell. At atmospheric pressure, the liquid crystal exhibited an isotropic to nematic phase transition at 37.3 °C which is close to the listed value of 36.8 °C. Over the temperature range 37.3 to 40.6 °C the coexistance curve is linear and has the slope $\Delta P/\Delta T = 2.8$ MPa/K. In typical operation the cell temperature was maintained at 38.7 °C which puts the nematic liquid crystal into the isotropic phase at atmospheric pressure. The transition to the nematic phase, for all the data described here, was induced by increasing the cell pressure form 0 to 6.9 MPa (1000 psi) in less than 8 msec.

Video microscopy was used to directly observe the defect tangle. The liquid crystal was viewed in transmission with an objective (Nikon, "E Plan", 4×, 0.1 NA) with a deep depth of field so that disclination lines throughout the sample would appear in focus. The sequence of photographs shown in Fig. 1 shows the coarsening of a defect tangle generated with the cell at 38.9 °C. Each picture shows a region about 500 μm across and is labeled with the time since the isotropic-to-nematic phase transition. Light propagates through the cell primarily by diffusion for times earlier than 3 sec. At 3 sec the mean free path is comparable to the sample cell thickness and a significant amount of light propagates through the cell without scattering. In

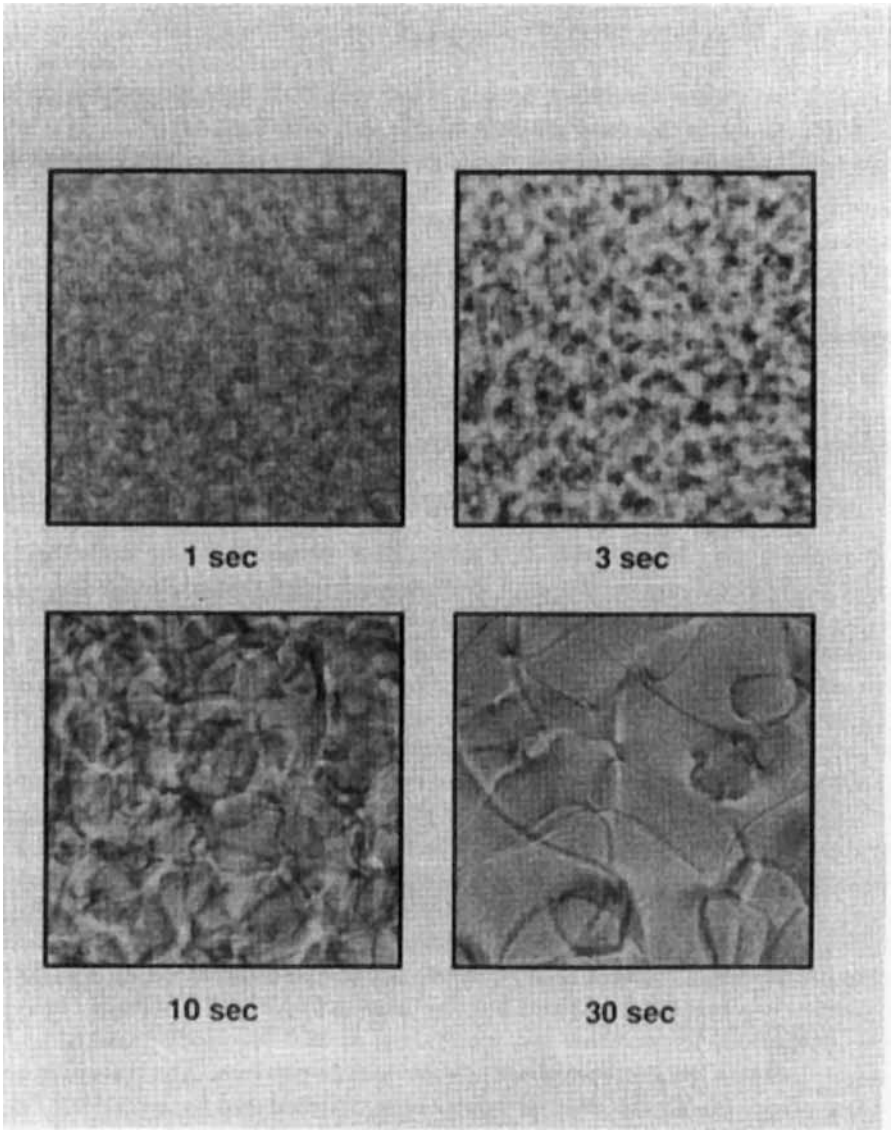

Figure 1: A sequence of pictures of the defect tangle in the nematic phase. Each frame is labeled with the time after the phase transition occured. After about three seconds light begins to penetrate the defect tangle without scattering.

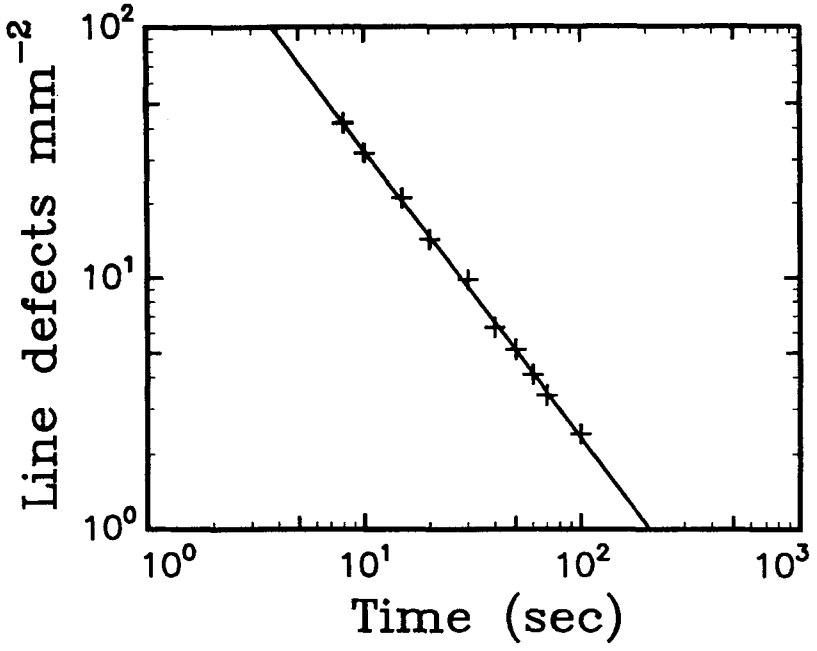

Figure 2: String density (line defects mm^{-2}), as measured by video microscopy, versus time. Data for a pressure jump from 0 to 6.9 MPa and a temperature of 38.9 ^0C are shown. The solid line is a least squares fit with a slope of -1.10±.06.

the frame at 10 sec the defect tangle has coarsened sufficiently that individual defect lines can be identified.

Video microscopy was used to record the coarsening of the defects. The recording was done at 200 frames/s using an HSV-400 (NAC, Inc.) video recorder. Fig. 2 is a log-log plot of the defect density versus time obtained by averaging the values obtained from nine separate runs. The defect density plotted is the number of type 1/2 disclination lines per unit area crossing a plane through the medium. This quantity was measured by counting the number of disclination lines crossing each of several planes, each measuring 1.36 mm by 0.45 mm (the visible width of the video frame by the cell depth) and is related to the defect density measured in line length per unit volume via a geometrical factor that depends on the details of the statistics of the string tangle. The least squares fit to these data gives $\rho_s \propto t^{-1.1}$ which is close to the expected scaling Eq.(2) for the string density. The uncertainty in the time measurement is less than 5 millisec and the statistical uncertainty in the defect density measurement is less than 5%.

Light transmission studies were performed by removing the cell from the microscope stage and mounting it on an optical bench. Linearly polarized light, with 638 nm wavelength, from a 0.5 mW polarization stablized He-Ne laser (Edmund Scientific, "Uniphase," #1508P-0) was passed through the cell. The laser light intensity was monitored by extracting some of the light via a 50-50 beam splitter placed between the laser and the sample cell. The output intensity of the laser and

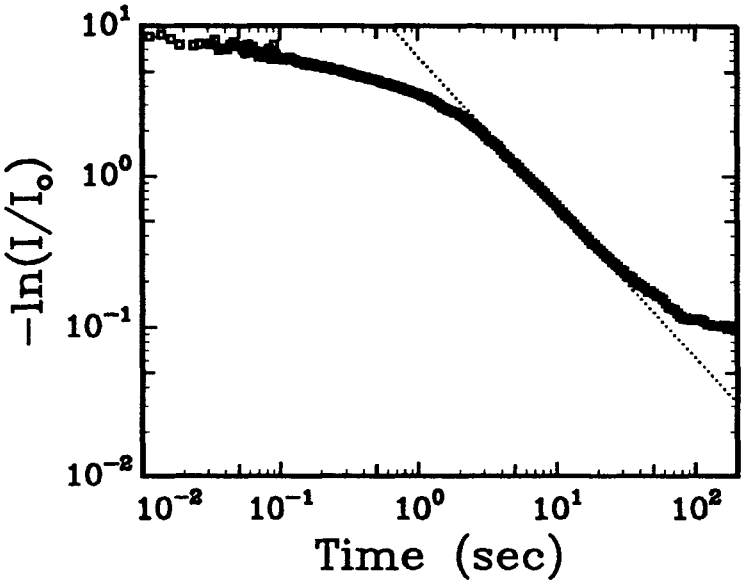

Figure 3: The late time coarsening of the defect density, measured by light transmission, shown as intensity versus time and plotted as $-\ln(I/I_0)$ versus time on a log-log scale. The dotted line has a slope of -1.0.

the light transmitted through the cell were simultaneously monitored with photodiodes (United Detector Tech., PIN-5DP). The photodiode outputs were amplified and recorded using a 12 bit A/D converter data acquisition card ("Labmaster" from Scientific Solutions). Fig. 3 through Fig. 5 show the averaged data taken from nine runs with the cell temperature at 38.7 °C. In these runs the time is measured with an accuracy of 3 milliseconds.

Fig. 3 shows $-\ln(I/I_0)$ versus time on a log-log plot. A least squares fit over the time interval from 3 sec to 20 sec gives a line with a slope of -0.93±.05. This is close to the expected scaling t^{-1} of Eq.(2). It is also close to the scaling $t^{-1.10}$ previously obtained by measuring the defect density directly. The value of the slope and the apparent behavior of $-\ln(I/I_0)$, particularly at late times, is sensitive to the measurement of I_0. The sensitivity to I_0 is considerably reduced by plotting $d[\ln(I/I_0)]/dt$ as a function of time. This quantity is proportional to $d\rho_s/dt$ and is thus expected to scale as t^{-2}. Fig. 4 shows $d[\ln(I/I_0)]/dt$ plotted as a function of time on a log-log plot. The data was obtained by numerically differentiating the data of Fig. 3. The measured scaling of this quantity, over the time interval of 3 to 30 sec, is $t^{-2.08}$, implying that the string density scales as $\rho_s \propto t^{-1.08}$.

From the expected early time scaling of the intensity Eq. (3) it follows that $d[\ln(I/I_0)]/dt$ should scale as

$$\frac{d}{dt}\ln(I/I_0) \propto t^{-1} \tag{7}$$

at early times. A dashed line of slope 1 is drawn in Fig. 4 to indicate this expected

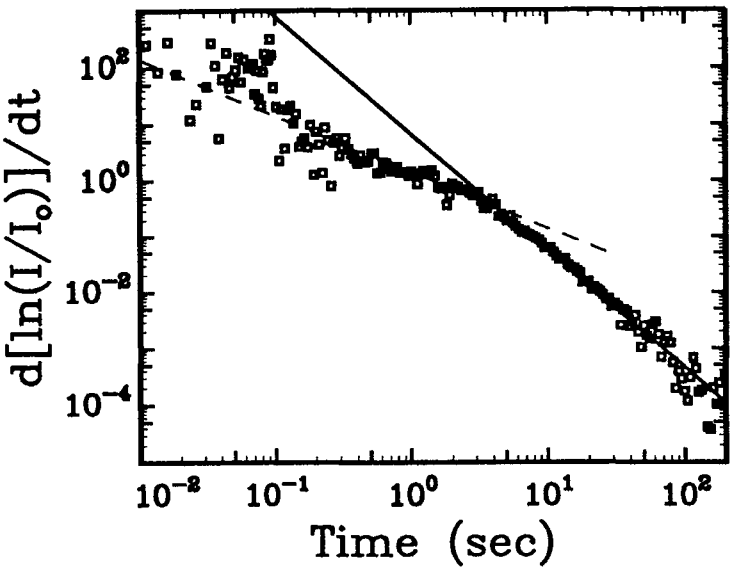

Figure 4: The derivative of the data shown in Fig. 3, $d[\ln(I/I_0)]/dt$, versus time on a log-log scale. The solid line is a least squares fit with a slope of -2.08±.27 and the dashed line indicates the expected early time coarsening, $I \propto t$.

scaling. A somewhat better way to display the early time scaling is to plot I/I_0 as a function of time on a log-log plot as shown in Fig. 5. The early time data should, according to Eq. (3), exhibit a slope of 1. The solid line is a least squares fit to the data over the time interval 10^{-2} sec < 1 sec. The line has a slope of 1.13±.07, close to the expected slope. The dashed curve is a fit of the late time intensity to $\ln(I/I_0) = -at^{-1}$ with $a = 5.75$. The "crossover" region, from early to late time coarsening, is only half a decade, spanning times from 1 to 3 sec.

Using light transmission we have followed for nearly four decades in time the annealing of line defects in a nematic liquid crystal. We have studied the annealing of line defects using light transmission. The liquid crystal trans(trans)-4-methoxy-4'-n-pentyl-1,1'-bicyclohexyl was used in these studies because of its low optical anisotropy. Two distinct scaling regimes for the light intensity were observed: an early time regime in which light propagates diffusively to the detector, and a late time regime in which unscattered light dominates the light reaching the detector. The scaling of the string density ρ, with time is within 10% of the expected scaling of $\rho \propto t^{-1}$ for both early and late times. Light transmission has thus proved to be a useful tool for probing the coarsening of nematic liquid crystals.

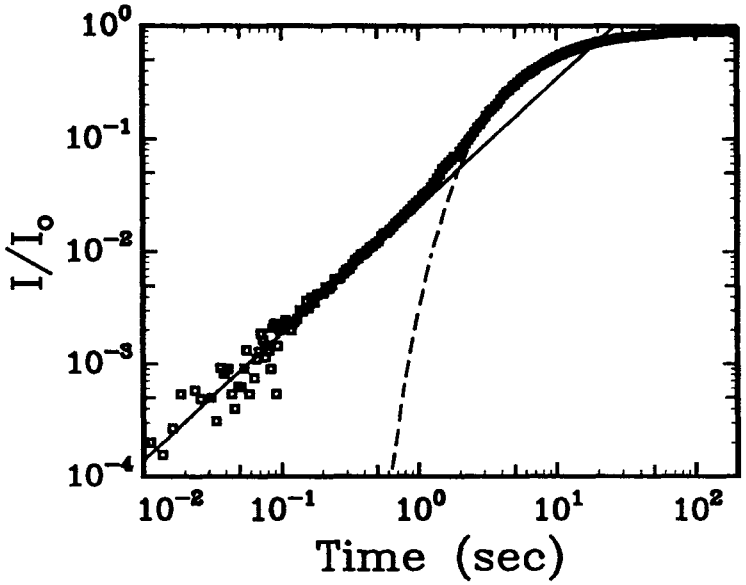

Figure 5: The early time coarsening, measured by laser transmission, displayed as I/I_0 versus time on a log-log scale. The solid line is a least squares fit with a slope of 1.13 $\pm$.07. The dashed line is a fit of $\ln(I/I_0)$ to the expected late time dependence, $-at^{-1}$.

References

1. I. Chuang, R. Durer, N. Turok, B. Yurke, Science **251**, 1336 (1991).
2. P. C. Hohenberg and B. I. Halperin, Rev. Mod. Phys. **49**, 435 (1977).
3. J. D. Gunton, M. San Miguel, and P. S. Sahni, in *Phase Transitions and Critical Phenomena*, edited by C. Domb and J. L. Lebowitz (Academic, London, 1983), p. 267.
4. H. Furukawa, Adv. Phys. **34**, 703 (1985).
5. P. W. Voorhees, J. Stat. Phys. **38**, 231 (1985).
6. Fong Lui, M. Mondello, and N. Goldenfeld, Phys. Rev. Lett. **66**, 3071 (1991).
7. M. Mondello and N. Goldenfeld, Phys. Rev. A **42**, 5865 (1990).
8. H. Toyoki and K. Honda, Prog. Theor. Phys. **78**, 237 (1987).
9. H. Toyoki, Phys. Rev. A **42**, 911 (1990).
10. H. Nishimori and T. Nukii, J. Phys. Soc. Jpn. **58**, 563 (1988).
11. R. Loft and T. A. DeGrand, Phys. Rev. B **35**, 8528 (1987).
12. F. de Pasquale and P. Tartaglia, Phys. Rev. B **33**, 2081 (1986).
13. G. F. Mazenko and M. Zannetti, Phys. Rev. B **32**, 4565 (1985).
14. A. Vilenkin, Phys. Rep. **121**, 263 (1985).
15. N. Turok, Phys. Rev. Lett. **63**, 2625 (1989).

16. C. T. Hill, D. N. Schramm, and J. N. Fry, Comments Nucl. Part. Phys. **19**, 25 (1989).
17. W. H. Press, B. S. Ryden, and D. N. Spergel, Astrophys. J. **347**, 590 (1989).
18. N. S. Manton, Phys. Rev. D **28**, 2019 (1983).
19. V. Kuzmin, V. A. Rubakov, and M. E. Shaposhnikov, Phys. Lett. B **155**, 36 (1985).
20. M. E. Shaposhnikov, Nucl. Phys. B **287**, 757 (1987) and **299**, 797 (1988).
21. N. Turok and J. Zadrozny, Phys. Rev. Lett. **65**, 2331 (1990).
22. M. Kléman, L. Michel, and G. Toulouse, J. de Physique **38**, L-195 (1977).
23. N. D. Mermin, Rev. Mod. Phys. **51**, 591 (1979).
24. L. Michel, Rev. Mod. Phys. **52**, 617 (1980).
25. H. Orihara and Y. Ishibashi, J. Phys. Soc. Jpn. **55**, 2151 (1986).
26. T. Nagaya, H. Orihara, and Y. Ishibashi, J. Phys. Soc. Jpn. **56**, 3086 (1987).
27. T. Nagaya, H. Hotta, H. Orihara, and Y. Ishibashi, J. Phys. Soc. Jpn. **60**, 1572 (1991).
28. T. Shiwaku, A. Nakai, H. Haswgawa, and T. Hashimoto, Polymer Commun. **28**, 174 (1987).
29. T. Shiwaku, A. Nakai, H. Hasegawa, and T. Hashimoto, Macromolecules **23**, 1590 (1990).
30. I. Chuang, N. Turok, B. Yurke, Phys. Rev. Lett. **66**, 2472 (1991).
31. G. W. Watson, Jr., P. A. Fleury, S. L. McCall, Phys. Rev. Lett. **58**, 945 (1987).